

Series vs Parallel Reflection-Type Phase Shifters

VITALY KIRILLOV^{1,2}, (Student Member, IEEE), DMITRY KOZLOV¹, (Member, IEEE),
AND SENAD BULJA¹, (Senior Member, IEEE)

¹Nokia Bell Labs, Dublin 15, D15 Y6NT Ireland

²Department of Microelectronics and Radio Engineering, Saint Petersburg Electrotechnical University "LETI," 197376 Saint Petersburg, Russia

Corresponding author: Vitaly Kirillov (vvkirillov@etu.ru)

ABSTRACT A performance comparison between series and parallel resonant circuits in the Reflection-Type Phase Shifter (RTPS) configuration is presented in this article. Initially, equations are derived to theoretically assess the fundamental limits of both configurations, in terms of the optimum values of the required resonant inductances and, subsequently, the maximum obtainable phase shifts of both configurations, as a function of the reactive parameters of the varactor diode. Then, based on these predictions, two sets of three RTPSs (three series-circuit and three parallel-circuit) operating at a center frequency of 2.3 GHz are designed, simulated, fabricated and their performance was measured and compared with the theoretically predicted results. For each set of the RTPS, the intrinsic parameters of the varactor diode (minimum capacitance and tuning ratio) are altered by the addition of a lumped element. This is done in order to adequately assess the performance of phase shifters for different characteristics of the active element. Then, based on the derived equations, the corresponding RTPS is designed so as to provide maximum phase shift. The theoretical analysis indicates that the parallel resonant configuration is inherently more capable of providing higher values of shift compared to its series resonant circuit counterpart, reaching 360° in the limit case. The measurement results largely confirm these theoretical findings, and the parallel RTPS configuration is shown to outperform the series RTPS configuration under most conditions. Results are discussed in detail.

INDEX TERMS Branch-line coupler, phase shifter, varactor.

I. INTRODUCTION

Phase shifters are one of the key elements in communication systems. The ability to control phase of a signal using voltage or current plays an important role in radar, phased-arrays, receiver systems and other types of beam-forming networks. Among all types of phase shifters RTPS, with inherently well-impedance matched inputs/outputs are of particular interest for applications where high phase shift values, excellent performance and small size are of importance.

The amount of obtainable phase shift from an RTPS is dependent on the structure of its reflective loads and its widespread use compared to its counterparts is evidenced by the wealth of the literature. The standard RTPS configuration consisting of varactor diodes in the circuits of the reflective loads [1] gives rather modest values of phase shift. These can be increased by resonating the varactor diode with a series

mounted inductor [2]. However, for phase shifts over 360° at least two varactor diode resonant circuits are necessary [3]–[6], typically realized with two series varactor diode-inductor connections mounted in parallel. The parallel connection between the varactor diode and the resonant inductor was mentioned in [7], however, no measured results were presented. As such, it is instructive to studiously examine the performance of the parallel-series configuration and compare it with its series configuration counterpart in the circuit of the reflective load.

In this article, we theoretically and experimentally examine the parallel resonant circuit in the RTPS configuration and compare it with its series resonant counterpart. We show that the parallel resonant circuit has inherent advantages over its series resonant circuit counterpart, by being capable of achieving much larger FoM in almost the entire range of maximum achievable phase shifts for different active component settings. Parallel resonant circuit RTPSs also have a better nonlinear performance, as will be demonstrated in the next sections.

The associate editor coordinating the review of this manuscript and approving it for publication was Lei Zhao¹.

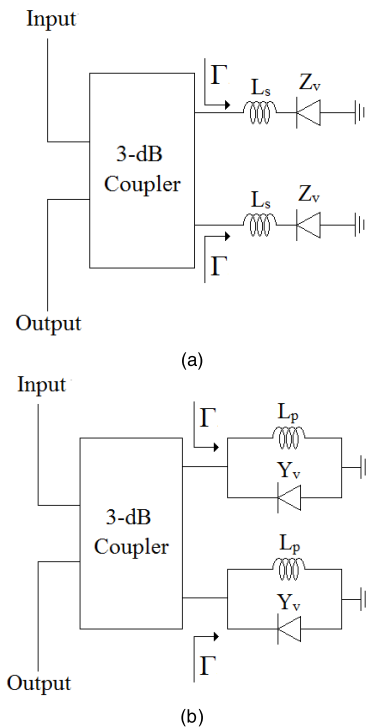


FIGURE 1. Reflection-type phase shifters with (a) series varactor-inductor and (b) parallel varactor-inductor configurations.

II. THEORY AND ANALYSIS

A. CASE OF SERIES CIRCUIT

With reference to Fig. 1 (a), and under the assumption of the ideal 3-dB coupler, the absolute value of the phase shift achievable can be written as [4]

$$\Delta\varphi = 2 \left[\arctan \left(\frac{Z_v \max}{Z_0} \right) - \arctan \left(\frac{Z_v \min}{Z_0} \right) \right], \quad (1)$$

where Z_0 stands for the characteristic impedance. The maximum value of the (1) is found by taking the first derivative of (1) with respect to L_s , to yield [4]

$$\Delta\varphi_s = 4 \arctan \left(\frac{1 - r_s}{2\omega C_{\min} r_s Z_0} \right) \quad (2)$$

obtained when the value of the inductor L_s is

$$L_s = \frac{r_s + 1}{2\omega^2 C_{\min} r_s} \quad (3)$$

In (2) and (3), ω stands for the angular frequency of operation, C_{\min} is the minimum capacitance of the varactor diode, while r_s is the capacitance ration of the varactor diode, given by $r_s = C_{\max}/C_{\min}$. It is obvious from (2) that the maximum phase shift obtainable from the circuit of Fig. 1 (a) increases as the capacitance ratio increase, however, for a sufficiently high values of r_s , a state of diminishing returns is reached, i.e. the maximum possible phase shift becomes

$$\begin{aligned} \Delta\varphi_s &= \lim_{r_s \rightarrow \infty} \left(4 \arctan \left(\frac{1 - r_s}{2\omega C_{\min} r_s Z_0} \right) \right) \\ &= 4 \arctan \left| \frac{1}{2\omega C_{\min} Z_0} \right|, \end{aligned} \quad (4)$$

which indicates that for high values of capacitance ratios, the maximum amount of obtainable phase shift becomes independent of r_s .

B. CASE OF PARALLEL CIRCUIT

With reference to Fig. 1 (b), and under the same assumptions as with the circuit of Fig. 1 (a), the absolute value of phase shift obtainable from this circuit is

$$\Delta\varphi_p = 2 \left[\arctan \left(\frac{Y_v \max}{Z_0} \right) - \arctan \left(\frac{Y_v \min}{Z_0} \right) \right] \quad (5)$$

The maximum amount of phase shift achieved using this circuit is

$$\Delta\varphi_p = 4 \arctan \left(\frac{\omega C_{\min} (r_p - 1)}{2Y_0} \right) \quad (6)$$

For the value of the inductor of

$$L_p = \frac{2}{\omega^2 C_{\min} (r_p + 1)} \quad (7)$$

In (6) and (7), ω stands for the angular frequency of operation, C_{\min} is the minimum capacitance of the varactor diode, r_p is the capacitance ration of the varactor diode, given by $r_p = C_{\max}/C_{\min}$ and Y_0 is the characteristic admittance of the circuit, given by $Y_0 = 1/Z_0$.

As opposed to the maximum phase shift obtainable using the series resonant circuit of (4), the maximum phase shift obtainable using the parallel circuit is not independent of the capacitance ratio, rather, for sufficiently large values of r_p , (6) becomes

$$\Delta\varphi_p = \lim_{r_p \rightarrow \infty} \left(4 \arctan \left(\frac{\omega C_{\min} (r_p - 1)}{2Y_0} \right) \right) = 2\pi, \quad (8)$$

i.e. a full 360° phase shift is obtainable using only one varactor diode - the result not achievable using a series resonant circuit.

It is now instructive to compare the performance of the two phase shifters for various values of C_{\min} and r_s (and, hence, r_p), so as to gain a better insight into their behavior. For this purpose, (4) and (8) are plotted against the typical values of C_{\min} and r_s (and, hence, r_p) in Figs. 2 and 3. For this purpose, the frequency of operation of 2.5 GHz is assumed operating in a standard 50-Ω system. Typical values of C_{\min} for a typical varactor diode lie in the range from 0.4 pF to 1 pF, while the maximum tuning ratios r_s (and, hence, r_p) can be as high as 10. Fig. 2 depicts the amount of phase shift obtainable from the series and parallel RTPS loads configurations as a function of the tuning ratio for three values of $C_{\min} = 0.4 \text{ pF}$, $C_{\min} = 0.7 \text{ pF}$ and $C_{\min} = 1 \text{ pF}$. Three conclusions can be drawn from this figure. First, the amount of phase shift obtainable from the series resonant circuit saturates relatively fast as a function of the tuning ratio. This is in opposition to the performance of the parallel resonant circuit, whose differential phase shift continues to increase even for high values of the tuning ratio. Second, the amount of phase shift obtainable from the series resonant circuit reduces as C_{\min} increases, while the opposite is true

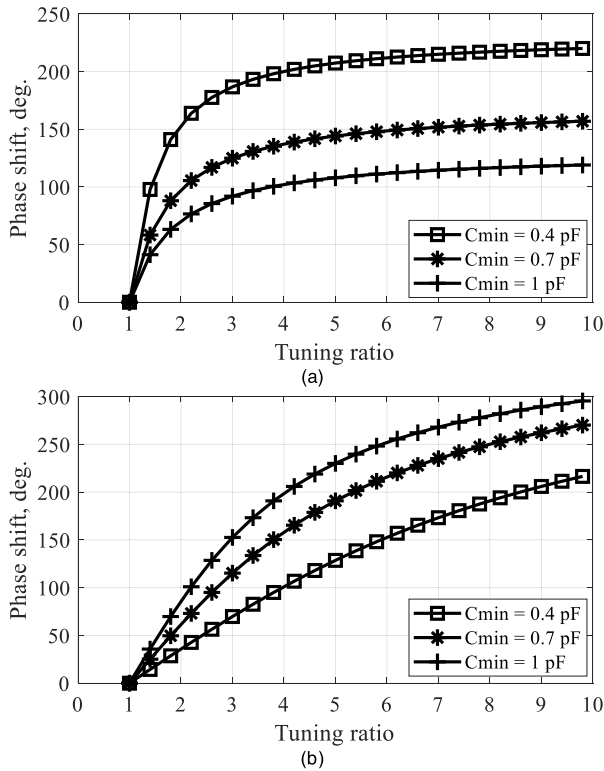


FIGURE 2. Phase shift as function of tuning ratio for different values of C_{min} ; for series (a) and parallel (b) resonant circuit.

for the parallel resonant circuit. Lastly and possibly most importantly, differential phase shift of the parallel resonant circuit is, in general, always greater than its series resonant circuit counterpart, with the exception for very small values of C_{min} for which they obtained phase shift values become comparable.

Similarly, Fig. 3 shows the achievable phase shift from both circuit configurations as a function of C_{min} , for three values of the tuning ratio, $r = 3$, $r = 7$ and $r = 10$. This figure complements the findings of Fig. 2, by showing that, in general, the series circuit configuration outperforms the parallel circuit configuration only for the cases of low values of C_{min} and low tuning ratios. The parallel circuit configuration offers a better performance for any other combination of C_{min} and the tuning ratio.

Several important conclusions can be drawn from Figs. 2 and 3. For the given parameters of a varactor diode in terms of its C_{min} and tuning ratio, it is possible to propose the optimum electrical circuit configuration, so as to achieve the highest possible values of phase shift. However, it is also equally important to realize that C_{min} and the tuning ratio can be altered by the addition of a lumped element. In this way, one can interpret such a combination as a varactor diode with an effective, equivalent C'_{min} and the tuning ratio.

C. CASE OF SERIES CONNECTION OF LUMPED ELEMENT AND VARACTOR DIODE

This is depicted in Fig. 4 for the cases when a capacitor and an inductor is added in series with a varactor diode.

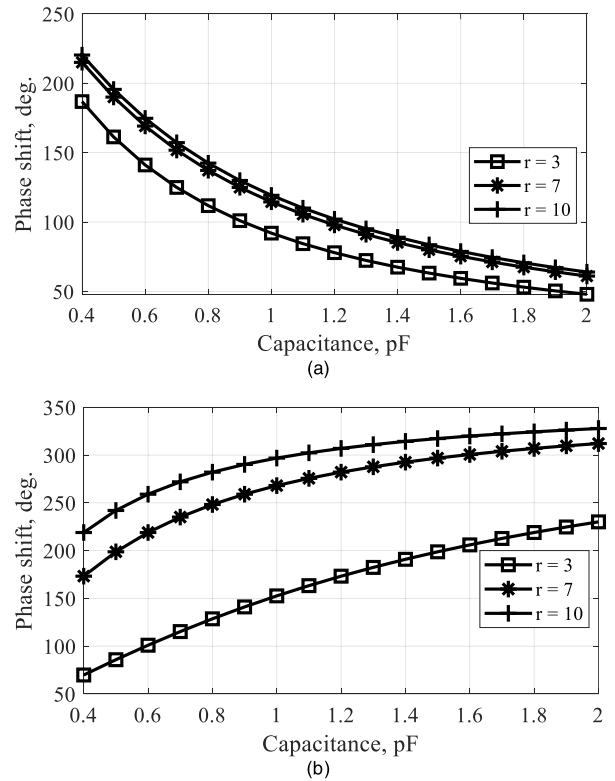


FIGURE 3. Phase shift as function of C_{min} for different values of tuning ratios; for series (a) and parallel (b) resonant circuit.

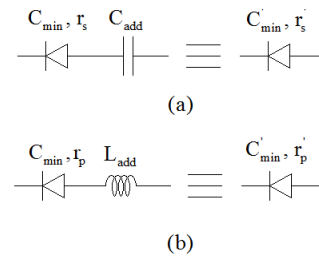


FIGURE 4. Effect of series addition of capacitor (a) and inductor (b) to varactor diode.

The addition of a capacitor, C_{add} , in series with a varactor diode, Fig. 4 (a) results in the reduction of equivalent C'_{min} but, it also reduces the equivalent tuning ratio, r'_s , in the following fashion

$$C'_{min} = \frac{C_{min}C_{add}}{C_{min} + C_{add}} \text{ and } r'_s = r_s \frac{C_{add} + C_{min}}{C_{add} + r_s C_{min}} \quad (9)$$

The equivalent varactor diode characteristics given by (9) are obviously not conducive to phase shift increase of the parallel resonant circuit configuration, since phase shift in this case increased by increasing the minimum capacitance and the equivalent tuning ratio. The exact effect of (9) on the series resonant circuit is somewhat uncertain, since (9) states that not only the minimum capacitance is reduced, but the tuning ratio too.

The addition of an inductor, L_{add} in series with a varactor diode, Fig. 4 (b) increases the equivalent C'_{min} and the

TABLE 1. Effect of addition of capacitor in series with varactor on optimum phase shifts from series and parallel resonant circuits.

C_{add} (pF)	C'_{min} (pF)	r'_s	Phase shift (series) (deg)	Phase shift (parallel) (deg)
0.5	0.2573	1.66	177	15
1	0.3464	2.16	178	35
1.5	0.3916	2.55	178	53
2	0.419	2.86	178	67
∞	0.53	5.6	178	172

TABLE 2. Effect of addition of inductor in series with varactor on optimum phase shifts from series and parallel resonant circuits.

L_{add} (nH)	C'_{min} (pF)	r'_s	Phase shift (series) (deg)	Phase shift (parallel) (deg)
0	0.53	5.6	178	172
0.25	0.5479	6.71	178	203
0.5	0.5671	8.39	178	229
1	0.6097	18.94	178	307
1.3	0.64	124.3	178	352

equivalent tuning ratio, r'_p in the following way

$$C'_{min} = \frac{C_{min}}{1 - \omega^2 L_{add} C_{min}} \text{ and } r'_p = r_p \frac{1 - \omega^2 L_{add} C_{min}}{1 - \omega^2 L_{add} r_p C_{min}} \quad (10)$$

for $\omega^2 L_{add} C_{min} r_p \leq 1$.

The equivalent diode characteristics given by (10) are favorable for phase shifting applications in the parallel resonant circuit, but not in the series resonant circuit, due to the fact that the addition of an inductor results in an increase in the minimum capacitance. Table 1 and 2 depict these scenarios for different values of C_{add} and L_{add} together with the influence of their addition on the achievable phase shift from the series and parallel resonant circuit configurations.

The varactor diode chosen for this purpose is from Macom [8] with a part number MAVR-00020. The capacitance parameters of this diode are $C_{min} = 0.53 \text{ pF}$ and tuning ratio of 5.6, while the frequency of operation of 2.5 GHz is assumed. Given the characteristics of the present diode, the condition of (10) is satisfied for the values of L_{add} lower than 1.35 nH.

Tables 1 and 2 indicate that the addition of a lumped element has no effect on the achievable phase shift from the series resonant circuit, however, it has a profound effect on the phase shift obtainable from the parallel resonant circuit. Therefore, the optimum RTPS configuration using a parallel resonant circuit is given in Fig. 5.

It can be observed from (10), that no optimum value of L_{add} exists; instead the value of L_{add} needs to be chosen in such a way so that it does not introduce significant, additional

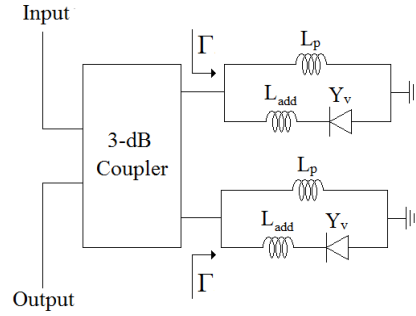


FIGURE 5. Optimum RTPS configuration using parallel resonant reflective loads.

TABLE 3. Parasitic parameters of the varactor diode mavr-000202.

R_d , Ohm	L_d , nH	C_d , pF
2.45	0.89	0.02

losses. For this purpose, the circuit of Fig. 5 needs to be closer analyzed.

For accurate analytical calculations, a diode model based on manufacturer’s specifications and the measurement results, was constructed, Fig. 6. The diode’s equivalent circuit contains nonlinear capacitance $C(V)$, parasitic inductance L_d , parasitic capacitance C_d arising from the packaging and internal leads, and resistor R_d , responsible for losses.

Non-linear capacitor $C(V)$ is described by the following formula [9]

$$C(V) = C_0 \left(1 - \frac{V}{V_j}\right)^{-M}, \quad (11)$$

where C_0 stands for the capacitance in zero voltage, V_j is the junction potential and M is the grading parameter. This equation fully describes the dependence of capacitance on voltage in the voltage range from 0 to 20 V.

For the analytical description, the input impedance of the parallel resonant circuit, containing inductances L_{add} , L_p , and the detailed diode model presented earlier, was calculated by using

$$Z_p(V) = \frac{\left(ZL_{add} + \frac{(ZC(V)+R_d+L_d)C_d}{ZC(V)+R_d+L_d+C_d} \right) ZL_p}{ZL_{add} + \frac{(ZC(V)+R_d+L_d)C_d}{ZC(V)+R_d+L_d+C_d} + ZL_p} \quad (12)$$

Phase shift is then calculated in the following manner

$$\Gamma_p(V) = \frac{Z_p(V) - Z_0}{Z_p(V) + Z_0}, \quad (13)$$

where $Z_0 = 50 \Omega$. The values of L_{add} and L_p are varied from 0 to 10 nH and from 0 to 20 nH, respectively, in 0.5 nH increments. For each pair of inductances, a corresponding value of phase shift defined as a difference between the phase shift at 0 V and 20 V is then found. This corresponds to the maximum value of phase shift obtainable from the selected pair of inductances. Maximum insertion loss was found in voltage range on a diode from 0 to 20 V with 1 V increment.

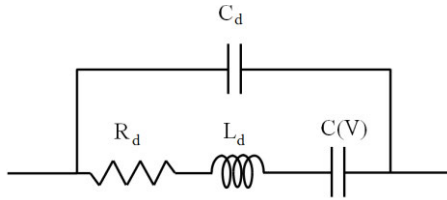


FIGURE 6. Varactor diode MAVR-000202 model.

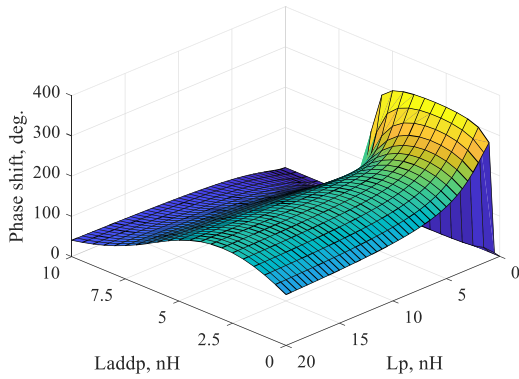


FIGURE 7. Calculated phase shift of RTPS with parallel resonant circuit at 2.5 GHz.

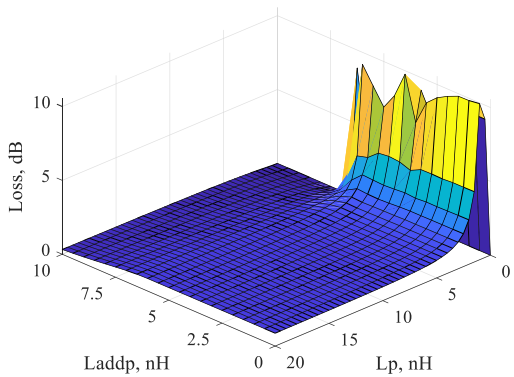


FIGURE 8. Calculated maximum insertion loss of RTPS with parallel resonant circuit at 2.5 GHz.

As a result, 3-D graphs of phase shift and insertion losses were plotted, as shown in Fig. 7 and Fig. 8, respectively. It can be seen from these figures, that maximum losses correspond to the maximum phase shift. In the design of phase shifters, the parameter of paramount importance is the ratio of obtainable phase shift and insertion loss; this parameter is referred to as Figure-of-Merit (FoM) and is given by

$$FoM = \frac{\Delta\varphi}{|S_{21}|} \left[\frac{\text{deg}}{\text{dB}} \right], \quad (14)$$

where $\Delta\varphi$ is maximum phase shift which we can achieve in voltage range from 0 to 20 V and $|S_{21}|$ is maximum loss in the same voltage range.

As evident, this parameter infers how much phase shift was achieved at the expense of insertion loss. For the RTPS parallel resonant circuit presented here, Fig 9 shows the obtained FoM. The maximum FoM of 205 deg/dB

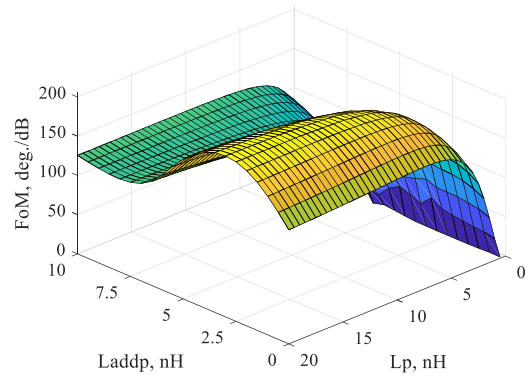


FIGURE 9. Calculated FoM of RTPS with parallel resonant circuit at 2.5 GHz.

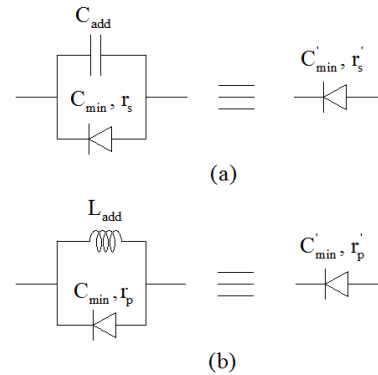


FIGURE 10. Effect of parallel addition of capacitor (a) and inductor (b) to varactor diode.

value for the presented phase shifter was obtained for the inductance values of $L_{add} = 3$ nH and $L_p = 20$ nH at 2.5 GHz.

D. CASE OF PARALLEL CONNECTION OF LUMPED ELEMENT AND VARACTOR DIODE

In a similar way as performed earlier, it is instructive to perform the analysis of the effect of the parallel lumped combination of the varactor diode and the lumped element, Fig. 10. The addition of a capacitor in parallel to the varactor diode results in the following, equivalent diode characteristics

$$C'_{min} = C_{min} + C_{add} \text{ and } r'_s = \frac{r_s C_{min} + C_{add}}{C_{min} + C_{add}} \quad (15)$$

The addition of a capacitor in parallel to the varactor diode results in the increase of the equivalent minimum capacitance, but it also results in the decrease in the tuning ratio. Such characteristics are not desirable in the design of RTPS, since they lead to the reduction of achievable phase shift.

Next, the parallel combination of an inductor and varactor diode is considered, Fig. 10 (b). The equivalent varactor parameters in this case become

$$C'_{min} = \frac{\omega^2 L_{add} C_{min} - 1}{\omega^2 L_{add}} \text{ and } r'_p = \frac{\omega^2 L_{add} r_p C_{min} - 1}{\omega^2 L_{add} C_{min} - 1} \quad (16)$$

for $\omega^2 L_{add} C_{min} > 1$.

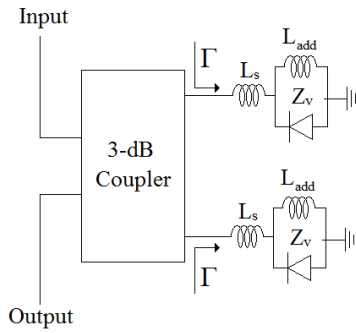


FIGURE 11. Optimum RTPS configuration using series resonant reflective loads.

TABLE 4. Effect of addition of capacitor in parallel with varactor on optimum phase shifts from series and parallel resonant circuits.

C_{add} (pF)	C'_{min} (pF)	r'_s	Phase shift (series) deg	Phase shift (parallel) (deg)
0	0.53	5.6	178	172
0.5	1.03	3.39	93	171
1	1.53	2.61	57	176
1.5	2.03	2.21	38	176
2	2.53	1.97	28	175

TABLE 5. Effect of addition of inductor in parallel with varactor on optimum phase shifts from series and parallel resonant circuits.

L_{add} (nH)	C'_{min} (pF)	r'_s	Phase shift (series) deg	Phase shift (parallel) (deg)
8	0.023	108	351	176
10	0.12	21.6	315	176
15	0.25	10.92	266	176
20	0.33	8.48	238	175
∞	0.53	5.6	178	172

Equation (16) indicates that as long as the reactance of the added inductor is greater than the reactance at the minimum capacitance, the reactance of the equivalent, minimum capacitance will always be capacitive. This condition is satisfied for the values of L_{add} greater than 7.64 nH. As such, the equivalent minimum capacitance can be made very low with a careful choice of the inductor L_{add} . The low values of C'_{min} in (16) will result in a considerable increase in the tuning ratio.

Tables 4 and 5 indicate the effect of the addition of a parallel lumped element on the obtained phase shift at 2.5 GHz. To be specific, the addition of a parallel capacitor to the varactor diodes is deleterious to the phase shift performance. The addition of the parallel inductor, however, has the potential to significantly increase the phase shift of the series resonant circuit by virtue of reducing the equivalent minimum capacitance and increasing the tuning ratio. The optimum RTPS configuration in this case is given in Fig. 11.

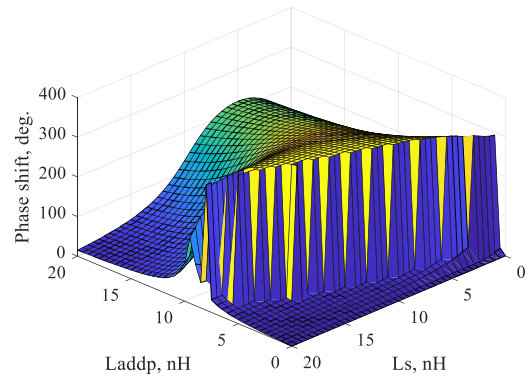


FIGURE 12. Calculated phase shift of RTPS with series resonant circuit.

Both RTPS circuits of Figs. 5 and 11 would provide a significant increase of phase shift than that available from using the RTPS circuits of Fig.1, for optimum values of L_s and L_p . However, it is important to realize, that, in general, inductors with high inductances should be avoided, due to their high parasitic resistance. Therefore, the preferable RTPS configuration is the one shown in Fig. 5, since only the modest values of additional inductors are needed. The input impedance of the RTPS with a series resonant circuit in its reflective loads can be analytically represented as

$$Z_s(V) = ZL_s + \frac{ZL_{add} \frac{(ZC(V)+R_d+L_d)C_d}{ZC(V)+R_d+L_d+C_d}}{ZL_{add} + \frac{(ZC(V)+R_d+L_d)C_d}{ZC(V)+R_d+L_d+C_d}} \quad (17)$$

The corresponding relationship for the phase shift becomes

$$\Gamma_s(V) = \frac{Z_s(V) - Z_0}{Z_s(V) + Z_0}, \quad (18)$$

where, as before, $Z_0 = 50 \Omega$. The 3-D graphs of the calculated phase shift, insertion loss, and FoM of the corresponding RTPS with a series resonant circuit are shown in Figs. 12-14. These figures indicate that the FoM of 180 deg/dB value for the presented phase shifter was obtained for the inductance values of $L_{add} = 20$ nH and $L_s = 3$ nH at the frequency of 2.5 GHz. For the given diode used in the present example, this infers that the parallel resonant RTPS outperforms its series resonant RTPS counterpart.

E. SERIES VS PARALLEL RESONANT CIRCUITS RTPS – LINEAR PARAMETERS

In order to provide a meaningful comparison between the RTPSs with series and parallel circuits, 3-D phase shift and FoM plots are used. For this purpose, phase shift plots were sliced at a constant phase plane. On every such plane the maximum FoM points were chosen, corresponding to minimum insertion loss for the achieved phase shift. As a result, the dependence of maximum FoM points against the achieved phase shift is obtained and the results are shown in Fig. 15.

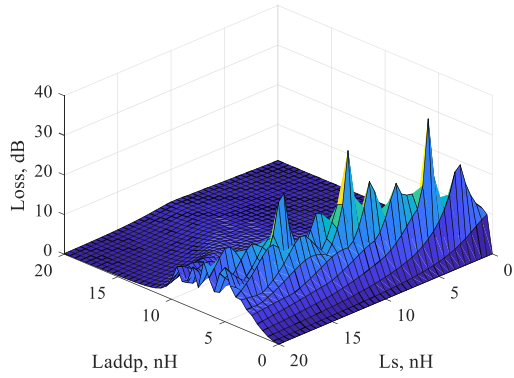


FIGURE 13. Calculated maximum insertion loss of RTPS with series resonant circuit at 2.5 GHz.

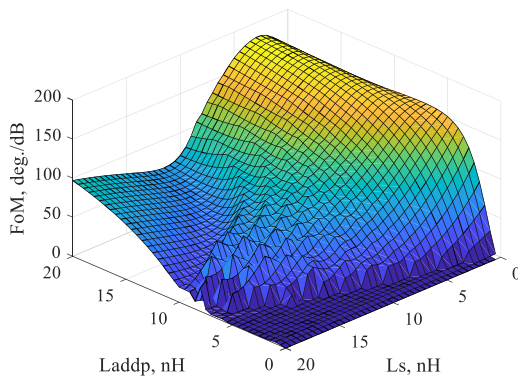


FIGURE 14. Calculated FoM of RTPS with series resonant circuit at 2.5 GHz.

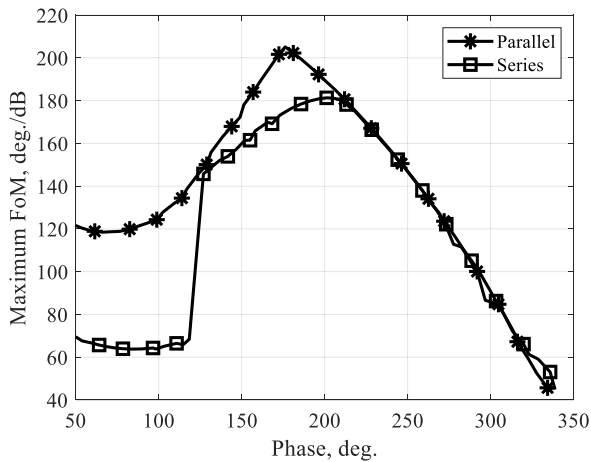
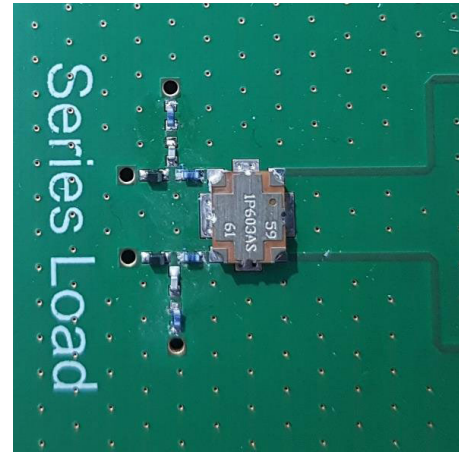


FIGURE 15. Calculated FoM for RTPS with series and parallel resonant circuits at 2.5 GHz.

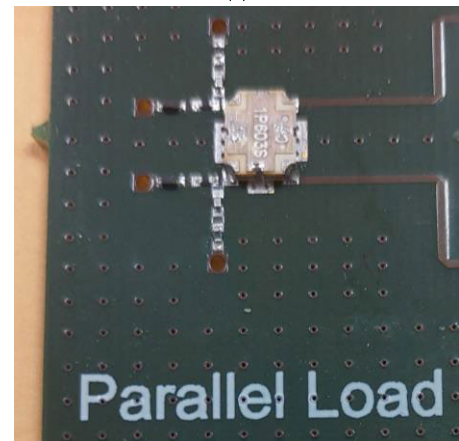
Based on Fig. 15, it can be concluded that RTPS with parallel circuit demonstrates better performance than the RTPS with a series circuit.

III. RESULTS

Based on the theory developed in the previous section, both series and parallel resonant reflection loads phase shifters



(a)



(b)

FIGURE 16. Manufactured (a) series RTPS and (b) parallel RTPS.

have been manufactured, Fig. 16. For the purpose of fabrication, the FR 4 substrate with $\epsilon_r = 4.3$ and the height of 0.38 mm was used. As a 3-dB coupler, a quadrature hybrid coupler from Anaren, 2 1P603S, was used for both type of phase shifters. According to the datasheet, this coupler operates across the frequency range from 2.3 to 2.7 GHz with a maximum insertion loss of 0.3 dB. Consequentially that 3-dB coupler potentially limits the operational bandwidth of the phase shifter. However, it should be noted that this coupler could be replaced by other ones with advanced characteristics [10], [11]. A varactor diode available from Macom [8] with a part number MAVR-000202 was used for both phase shifting circuits, as indicated in the simulations. All used components and manufactured PCB have their own parasitic parameters, especially parasitic inductances, which will negatively affect the RF performance. For a better comparison with the experiments, small-signal simulations with S-parameters of all used components were carried out.

A. CASE OF RTPS WITH A SERIES LC RESONANT CIRCUIT – LINEAR PARAMETERS

The linear performance of both phase shifting circuits was recorded using a R&S ZNB8 Vector Network Analyzer

TABLE 6. Inductor values for experiment and simulations.

L_{add} (nH)	C'_{min} (pF)	r'_s	Phase shift (series) deg	Phase shift (parallel) (deg)
8	0.023	108	351	176
10	0.12	21.6	315	176
15	0.25	10.92	266	176
20	0.33	8.48	238	175
∞	0.53	5.6	178	172

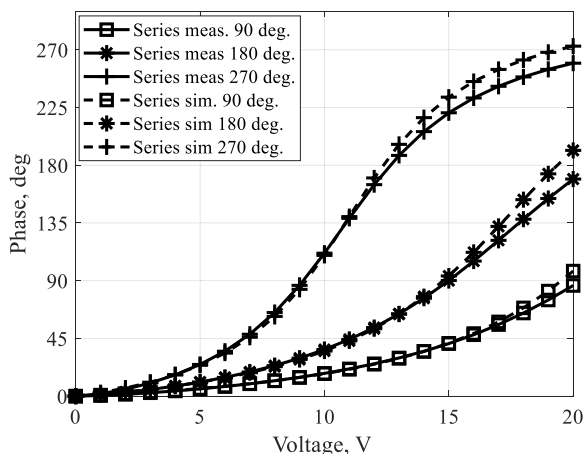


FIGURE 17. Simulated at 2.4 GHz (dotted line) and measured at 2.3 GHz (solid line) phase shift of RTPS with series resonant circuit normalized to 0 V phase shift.

(VNA), and the R&S HMP4030 power supply. The measurements were performed in the frequency range from 2 to 3 GHz as a function of the applied dc bias voltage, varying from 0 to 20 V in 1 V increments. For the purpose of the experiment 5 sets of inductances of L_{addp} and L_p and L_{adds} and L_s are used for the corresponding parallel and series RTPS, respectively. Table 6 shows the theoretical values of inductances as obtained through analytical calculations needed to obtain the corresponding phase shift values. In order to obtain these values, the closest inductances from Coilcraft [12] 0402HP series were chosen for the experiment, so as to obtain measured phase shifts as close as possible to the ones theoretically predicted, Table 6. The diode was biased using a bias tee, inferring that no dc bias circuitry was needed. However, the series resonant RTPS has an inductor in parallel with the varactor diode that will result in a short circuit at dc bias voltages. To prevent this, a DC block capacitor with $C = 22$ pF is added in series with the inductor. In this way, the application of the dc bias voltage on the varactor diode is enabled, while maintaining the optimum connection of the inductor and the diode.

The measured and simulated achieved phase shifts for the series RTPSs for maximum phase shift values of 90° , 180° and 270° are shown in Fig. 17. After taking into consideration all the parasitic effects of the PCB and the lumped elements in the simulations, the frequency of operation has shifted from

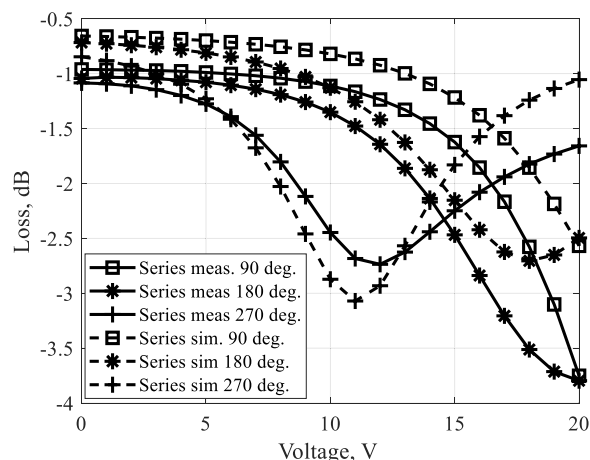


FIGURE 18. Simulated at 2.4 GHz (dotted line) and measured at 2.3 GHz (solid line) insertion loss of RTPS with series resonant circuit.

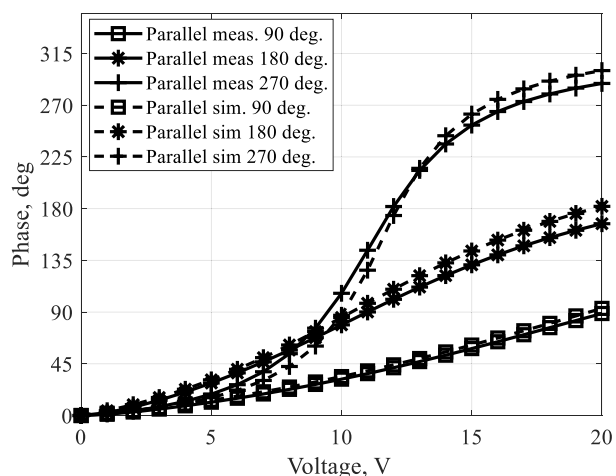


FIGURE 19. Simulated at 2.4 GHz (dotted line) and measured at 2.3 GHz (solid line) phase shift of RTPS with parallel resonant circuit normalized to 0 V phase shift.

the theoretically predicted 2.5 GHz to 2.4 GHz. Furthermore, the measured response has experienced a further downward shift to 2.3 GHz, compared to the simulations. This could be explained by the increased values of the inductances due to soldering and components value scatter.

A comparison between the measured and simulated phase shift responses of the series RTPS is presented in Fig. 17. Here, the solid line refers to the measured results, while the dotted line refers to its simulated counterpart. Similarly, Fig. 18 shows its insertion loss performance. As one can see, an excellent agreement between the predicted and measured performance was achieved.

B. CASE OF RTPS WITH A PARALLEL LC RESONANT CIRCUIT - LINEAR PARAMETERS

The parallel resonant RTPS of Fig. 5 is, just like its series resonant circuit counterpart, dc biased using a bias tee, which obviates the need for the dc bias circuitry. To prevent a short circuit from inductor in a parallel circuit, a DC block

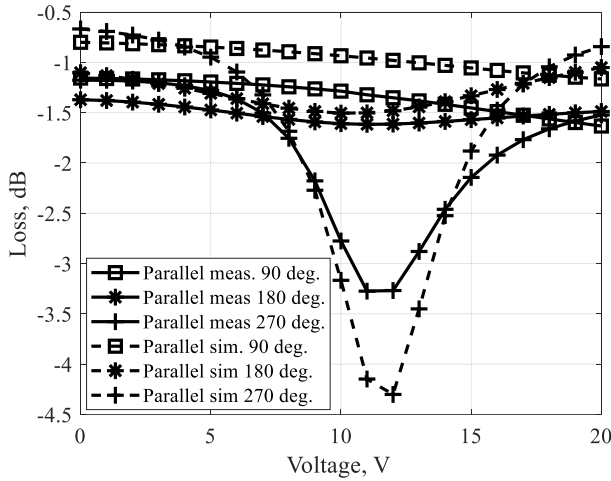


FIGURE 20. Simulated at 2.4 GHz (dotted line) and measured at 2.4 GHz (solid line) insertion loss of RTPS with parallel resonant circuit.

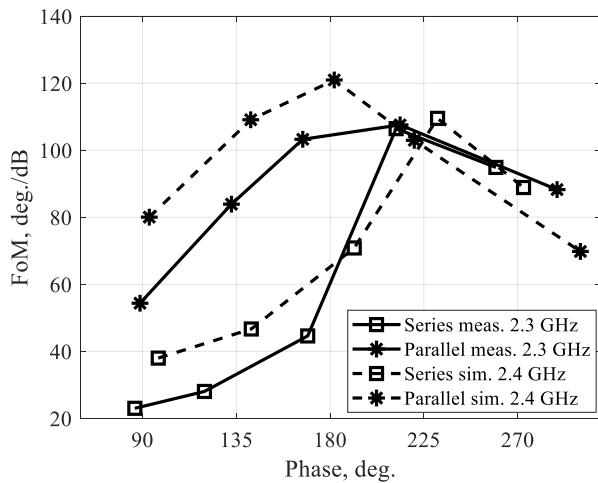


FIGURE 21. Simulated at 2.4 GHz (dotted line) and measured at 2.3 GHz (solid line) FoM performance of series and parallel RTPS circuits.

capacitor with $C = 22$ pF is added in series with the inductor like in a series RTPS circuit.

The measured and simulated phase shifts obtained from this configuration for 90° , 180° and 270° phase shift are shown in Fig. 19, for different dc bias voltages. Fig. 20 shows the corresponding insertion loss performance. The FoM performance of both circuits is shown in Fig. 21. This figure indicates that the FoM of the parallel circuit either better or similar to its series circuit counterpart. As can be seen from this figure, a good agreement between the simulated and measured performance was achieved. According to measurements both circuits have a maximum FoM of 107 deg/dB value for the maximum phase shift of 220 deg.

C. SERIES VS PARALLEL RESONANT CIRCUITS - NONLINEAR PARAMETERS

Nonlinear performance of both phase shifters is considered next. For this purpose, two tones at the frequencies of

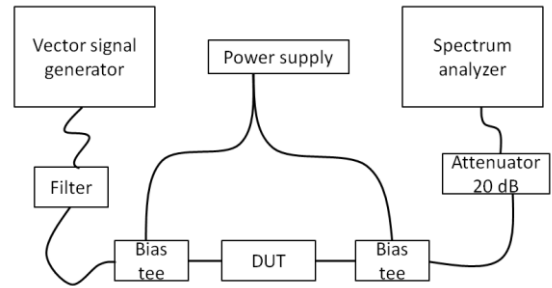


FIGURE 22. Block diagram of IM3 measurement setup.

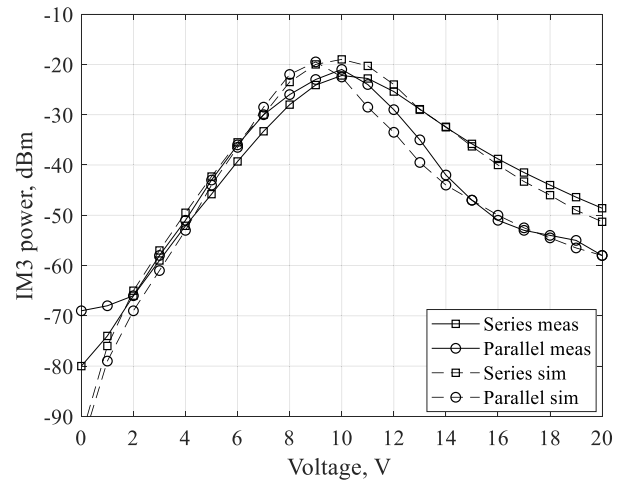


FIGURE 23. Simulated (dotted line) and measured (solid line) IM3 performance of phase shifters at input power $P_{in} = 15$ dBm as function of applied dc bias voltage.

$f_1 = 2.16$ GHz and $f_2 = 2.19$ GHz respectively, were applied to both phase shifters. The level of generated IM3 was monitored at the frequency of $2f_2 - f_1 = f_{IM3} = 2.22$ GHz. The IM3 generated by the source was suppressed by a band pass filter with a pass-band ranging from 2.13 - 2.19 GHz, with a suppression level at the frequency of f_{IM3} of $S_{21} = -30$ dB. The IM3 measurement block diagram is shown in Fig. 22.

For the purpose of the nonlinear measurements, the RTPS with series and parallel resonant circuits, both capable of exhibiting a phase shift of 270° are used. To achieve this phase shift corresponding values of inductances from table 6 were chosen. Fig. 23 shows the level of generated IM3 as a function of the applied dc bias voltage for an input power level of $P_{in} = 15$ dBm. Conversely, Fig. 24 shows the level of generated IM3 at a dc bias voltage of 10 V, as function of input power, P_{in} .

Fig. 23 indicates that the IM3 level of both phase shifters is dependent on the applied dc bias voltage. This figure shows that the level of generated IM3 initially increases for both phase shifters and peaks at a dc bias voltage of about 10 V, where the level of IM3 of both circuits is approximately -20 dBm. Beyond the dc bias of 10 V both phase shifters exhibit a reduction in the generated IM3 levels, with the

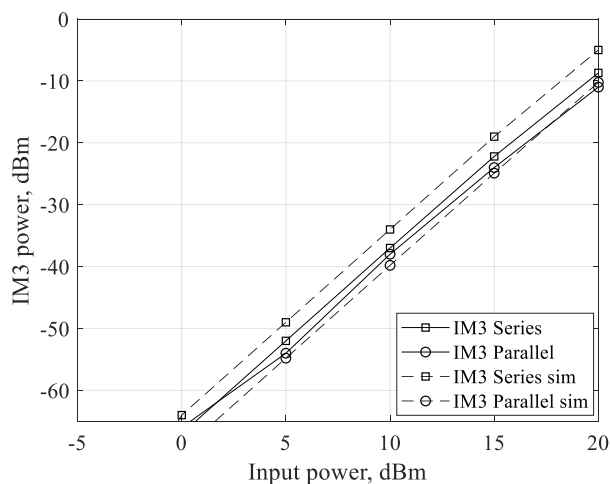


FIGURE 24. Simulated (dotted line) and measured (solid line) IM3 performance of phase shifters at dc bias of 10 V as function of the input power.

parallel circuit RTPS generally acquiring lower IM3 levels compared to its series circuit counterpart approximately after 10 V dc bias. Ultimately, at the highest allowable dc bias voltage of 20 V, the level of IM3 of the parallel circuit is about 10 dBm lower than that of the series circuit RTPS. Fig. 24 shows the IM3 dependence on input power, P_{in} , recorded at a dc bias of 10 V.

It is obvious from Figs. 23 and 24 that there is no clear winner with respect to the IM3 performance. The parallel resonant RTPS outperforms the series circuit RTPS for the dc bias voltages higher than 10 V, while for the applied dc bias voltages below 10 V, the levels of generated IM3 are very similar. It is, however, fair to say that the IM3 performance of the parallel circuit RTPS is marginally better than its series circuit counterpart. And, if one takes the superior linear performance of the parallel RTPS circuit into account, the overall performance winner is undoubtedly the parallel RTPS.

IV. CONCLUSION

In this article, a performance comparison of the proposed parallel circuit RTPS and the standard series circuit RTPS is presented. For the purpose of the fair comparison, both circuits are optimized to provide highest possible phase shifts. For this purpose, the equations enabling the maximum phase shift for the parallel and series resonant circuits of RTPS have been derived.

Both phase shifters have been designed, fabricated and their performance was measured in the frequency range 2 GHz – 3 GHz. The parallel RTPS configuration is capable of much higher phase shifts compared to its series RTPS counterpart. For the given varactor diode, the maximum, theoretically 205 deg/dB, while the maximum theoretical FoM of the series RTPS is 180 deg/dB.

For the purpose of the measurements, several optimal RTPS configurations using different values of inductances with both the series and parallel circuits have been analyzed.

Here, it is shown that the parallel circuit configuration achieves much higher FoM compared to the series circuit counterpart for phase shifts up to 220°, indicating its superiority. Above the phase shift values up to 220°, the FoM of both circuits are similar. The nonlinear results indicate that the level of generated IM3 of both phase shifters is dc bias dependent and, while the IM3 curves of both devices follow the same trend, the parallel RTPS circuit configuration shows lower IM3 levels for the dc bias voltages higher than 10 V. Below the dc bias of 10 V, the IM3 levels of both phase shifters are very similar.

Finally, taken holistically, the parallel circuit RTPS is an obvious winner – for the given diode and the amount of real estate it offers higher FoM, while delivering almost similar non-linear performance.

REFERENCES

- [1] R. N. Hardin, E. J. Downey, and J. Munushian, "Electronically variable phase shifter utilizing variable capacitance diodes," *Proc. IRE*, vol. 48, no. 5, pp. 944–945, 1960.
- [2] R. M. Searing, "Variable capacitance diodes used as phase-shift devices," *Proc. IRE*, vol. 49, pp. 640–641, Mar. 1961.
- [3] R. V. Garver, "360° varactor linear phase modulator," *IEEE Trans. Microw. Theory Techn.*, vol. MTT-17, no. 3, pp. 137–147, Mar. 1969.
- [4] F. Ellinger, R. Vogt, and W. Bachtold, "Ultra-compact reflective-type phase shifter MMIC at C-band with 360° phase-control range for smart antenna combining," *IEEE J. Solid-State Circuits*, vol. 37, no. 4, pp. 481–486, Apr. 2002.
- [5] C.-S. Lin, S.-F. Chang, and W.-C. Hsiao, "A full-360° reflection-type phase shifter with constant insertion loss," *IEEE Microw. Wireless Compon. Lett.*, vol. 18, no. 2, pp. 106–108, Feb. 2008.
- [6] J.-C. Wu, T.-Y. Chin, S.-F. Chang, and C.-C. Chang, "2.45-GHz CMOS reflection-type phase-shifter MMICs with minimal loss variation over quadrants of phase-shift range," *IEEE Trans. Microw. Theory Techn.*, vol. 56, no. 10, pp. 2180–2189, Oct. 2008.
- [7] T.-W. Li and H. Wang, "A millimeter-wave fully integrated passive reflection-type phase shifter with transformer-based multi-resonance loads for 360° phase shifting," *IEEE Trans. Circuits Syst. I, Reg. Papers*, vol. 65, no. 4, pp. 1406–1419, Apr. 2018.
- [8] (2019). [Online]. Available: <https://www.macom.com>
- [9] G. Massobrio and P. Antognetti, *Semiconductor Device Modeling with SPICE*, 1st ed. New York, NY, USA: McGraw-Hill, Dec. 1998.
- [10] P. Turalchuk, "Broadband small-size LTCC directional couplers," in *Proc. 40th Eur. Microw. Conf.*, Paris, France, Sep. 2010, pp. 1162–1165, doi: 10.23919/EUMC.2010.5616252.
- [11] D. A. Letavin, "Design of broadband branch-line coupler based on compact structure," in *Proc. Radiat. Scattering Electromagn. Waves (RSEMW)*, Divnomorskoe, Russia, Jun. 2019, pp. 168–170, doi: 10.1109/RSEMW.2019.8792803.
- [12] (2019). [Online]. Available: www.coilcraft.com



VITALY KIRILLOV (Student Member, IEEE) received the B.Sc. and M.Sc. degrees in radio engineering from Saint Petersburg Electrotechnical University "LETI," Saint Petersburg, Russia, in 2016 and 2018, respectively, where he is currently pursuing the Ph.D. degree with the Department of Microelectronics and Radio Engineering. In 2019, he had a six-month internship at Nokia Bell Labs, Dublin, Ireland. His primary research interests include microwave and antenna theory, synthesis of antennas, antenna arrays, and design of power amplifiers.



DMITRY KOZLOV (Member, IEEE) received the B.Sc. and M.Sc. degrees in radiophysics from Saint Petersburg Electrotechnical University “LETI,” Saint Petersburg, Russia, in 2009 and 2011, respectively, and the Ph.D. degree in electronics and electrical engineering from Queen’s University Belfast (QUB), Belfast, U.K., in 2016. He was a Marie Curie Early Stage Researcher with the Institute of Electronics, Communications and Information Technology, QUB, from 2013 to 2016. He is currently with Nokia Bell Labs, Dublin, Ireland. His primary research interests include microwave and antenna theory, including synthesis of antenna arrays, mechanisms of PIM generation in microwave passive and tunable devices, and wireless energy transfer systems.



SENAD BULJA (Senior Member, IEEE) received the B.Eng. (Hons.) and Ph.D. degrees from the University of Essex, Colchester, U.K., in 2002 and 2007, respectively. From 2007 to 2010, he was a Senior Research Officer with the School of Computer Science and Electronic Engineering, University of Essex, where he led the characterization effort of liquid crystals at microwave and millimeter-wave frequencies and the development of liquid-crystal-based millimeter-wave devices. Since 2010, he has been with Nokia Bell Labs, where he is currently a Senior Research Scientist. Here, he led the research effort in the design of low-profile resonators and filters and the discovery of dielectric tunability of inorganic electrochromic materials. He has authored/coauthored over 60 papers in international journals and conference proceedings and holds over 70 patents in the area of electromagnetics and telecommunications. His current research interests include new tunable RF dielectric and optical media, RF filters, RF amplifiers, specialized antennas, complete RF transceivers, and a plethora of RF passive and active devices (attenuators, couplers, and phase shifters) up to 240 GHz.

• • •